

The University of Akron IdeaExchange@UAkron

Honors Research Projects

The Dr. Gary B. and Pamela S. Williams Honors
College

Spring 2016

Assessing the Expression of Astrocytic Markers in Retinal Ganglion Cell Projection of LCR/HCR Rats

Isabella K. Bartholomew
The University of Akron, ikb1@zips.uakron.edu

Samuel Crish
Northeast Ohio Medical University, scrish@neomed.edu


James Holda
The University of Akron, holda1@uakron.edu

Jordan Renna
The University of Akron, jrenna@uakron.edu

Gina Wilson
Northeast Ohio Medical University, gwilson12@kent.edu

Please take a moment to share how this work helps you [through this survey](#). Your feedback will be important as we plan further development of our repository.

Follow this and additional works at: http://ideaexchange.uakron.edu/honors_research_projects

 Part of the [Disease Modeling Commons](#), [Eye Diseases Commons](#), [Molecular and Cellular Neuroscience Commons](#), [Nutritional and Metabolic Diseases Commons](#), and the [Pathological Conditions, Signs and Symptoms Commons](#)

Recommended Citation

Bartholomew, Isabella K.; Crish, Samuel; Holda, James; Renna, Jordan; and Wilson, Gina, "Assessing the Expression of Astrocytic Markers in Retinal Ganglion Cell Projection of LCR/HCR Rats" (2016). *Honors Research Projects*. 332.

http://ideaexchange.uakron.edu/honors_research_projects/332

This Honors Research Project is brought to you for free and open access by The Dr. Gary B. and Pamela S. Williams Honors College at IdeaExchange@UAkron, the institutional repository of The University of Akron in Akron, Ohio, USA. It has been accepted for inclusion in Honors Research Projects by an authorized administrator of IdeaExchange@UAkron. For more information, please contact mjon@uakron.edu, uapress@uakron.edu.

THE UNIVERSITY OF AKRON WILLIAMS HONORS COLLEGE

Assessing the Expression of Astrocytic Markers in Retinal Ganglion Cell Projection of LCR/HCR Rats

Honors Research Project

Isabella K. Bartholomew

4/22/2016

Dr. Samuel Crish, Northeast Ohio Medical University

Dr. James Holda, The University of Akron Biology Department

Dr. Jordan Renna, The University of Akron Biology Department

Gina Wilson BS, PhD Candidate, Northeast Ohio Medical University

Assessing the Expression of Astrocytic Markers in Retinal Ganglion Cell Projection of LCR/HCR Rats

Abstract

Metabolic Syndrome is a human condition that presents with various metabolic issues such as abnormal distribution of body fat, high blood pressure, and a prothrombotic state, among other problems (Alberti, et al, 2005). This syndrome is a risk factor for visual disorders, such as glaucoma, and is often associated with increased levels of neuroinflammation. Currently, the animal model used to replicate this syndrome is The Low Capacity Runner and High Capacity Runner Rat Model. These rats have been bred based on their running capacities for 30+ generations to have drastic metabolic differences. We assessed key areas of the retinal ganglion cell projection (optic nerve, superior colliculus, and retina) and other important thalamic nuclei in Metabolic Syndrome such as the arcuate nuclei and inferior colliculus, in the rats for expression of glial fibrillary acidic protein and Aquaporin 4. We expected to find elevated glial fibrillary acidic protein and Aquaporin 4 in key visual structures of Low Capacity Runner compared to High Capacity Runner rats. We found that in the superior colliculi of the Low Capacity Runner rats there was significantly a greater percent area fraction of glial fibrillary acidic protein than in the High Capacity Runner rats; as there was little Aquaporin 4 staining in many of the regions assessed, that data was inconclusive and it appears Aquaporin 4 plays a negligible role in stress-related changes associated with the Metabolic Syndrome phenotype. In this research, we provide novel evidence that Low Capacity Runner rats express an elevated immune response compared to their High Capacity Runner counterparts and that this response is partially specific to visual structures, as the inferior colliculus, an auditory-related thalamic nuclei, showed astroglial differences between High Capacity Runners and Low Capacity Runners. These findings could lead to a better understanding of the metabolic underpinnings of optic neuropathies and present new avenues for their treatment.

1. Introduction

In the media and modern society, there seems to be a fixation with weight loss and metabolism, especially with the advent of greater understanding of Metabolic Syndrome. Metabolic Syndrome (MetS) is a condition characterized by abnormal body fat distribution, insulin resistance, atherogenic dyslipidemia, elevated blood pressure, proinflammatory state, and prothrombotic state (Alberti, et al, 2005). With the growing epidemic in the United States of obesity, diabetes and pre-diabetes, there are a variety of comorbidities with these diseases including visual disorders such as glaucoma and diabetic retinopathy. While the effects of MetS have been quite heavily studied in the context of cardiovascular disease, skeletal muscle, and liver injury/steatosis, less work has been done to characterize its effects on the visual projection (Morris et al. 2014 and De Marco et al. 2012).

To study MetS in the laboratory, we use the LCR/HCR rat model. LCR/HCR rats are bred based on phenotypic running capacity to be either low capacity runners (LCR) or high capacity runners (HCR) (described by Koch & Britton, 2001; Koch, Britton & Wislof, 2012). HCR rats are naturally better runners, with lower resting blood glucose, higher percentage of lean body mass, and with higher levels of energy, while LCR rats, in opposition, have features typical of a pre-diabetic, metabolic syndrome state with elevated fat mass, elevated cholesterol and triglycerides as well as dysregulated blood glucose, and lower energy levels. HCR rats are far more active, spending more time each day running around their enclosures while the LCR rats limit movement and energy expended. LCR/HCR rats have been bred out over 30 generations to have this drastic, phenotypic metabolic difference. Even for an HCR rat that is the same weight as an LCR rat, the HCR rat would be more ambulatory and more active per minute than the LCR rat (Novak et al, 2009).

Astrocytes are pivotal in the maintenance of Central Nervous System homeostasis (Bondan, Martins, and Viani, 2013). Glial fibrillary acidic protein (GFAP) is a cytoskeletal marker expressed in astrocytes and will provide information on astrocytic number, distribution and activation status. Additionally, GFAP is found to be decreased for diabetic rats compared to healthy rats in scenarios of brain injury (Bondan, Martins, and Viani, 2013). Given the prevalence of visual disorders, like glaucoma, coinciding with metabolic dysfunction we hypothesized that there would be baseline differences between visual structures of HCR and LCR rats in absence of other experimental manipulations. Specifically, since elevated immune system modulators such as glial and astroglial reactivity is common among compromised and diseased visual structures, we hypothesized an increase in GFAP signaling in LCRs compared to HCRs. Aquaporin-4 (AQ4) is a water-channel protein that is upregulated in brain injury as well as neurodegeneration and downregulated in epilepsy, traumatic brain injury, and models of Alzheimer's disease (Ceccariglia et al., 2014, Nagelhus and Ottersen, 2013). Additionally, we hypothesized an increase in AQ4 on astrocytes as this water channel is upregulated under injured and stressed states. For example, in situations of neuroinflammation, the deletion of the AQ4 gene in mice causes them to have less of an inflammatory response than wild type mice when lipopolysaccharide was injected into the brain. In mice with the AQ4 gene, they also show impaired migration of reactive astroglia at sites of injury and impaired glial scar formation (Nagelhus and Otterson, 2013). Since glaucomatous neurodegeneration is often associated with changes in metabolism, the LCR/HCR rats could provide better insights into early identification of pathologies in the eyes or brain due to metabolic differences. These rats could also be used to help identify potential metabolic factors that may put some people (especially those who present with MetS) at increased risk for developing retinal pathologies.

2. Materials and Methods

2.1. Animals

The LCR-HCR rat model of metabolic syndrome was funded by the National Center for Research Resources grant R24 RR017718 and is available for collaborative study from University of Michigan. These rats are bred based on phenotypic running capacity to be either low capacity runners or high capacity runners (described by Koch & Britton, 2001; Koch, Britton & Wislof, 2012). The HCR rats are naturally better runners, with lower resting blood glucose, and higher percentage of lean body mass while LCR rats, in opposition, have features typical of a pre-diabetic, metabolic syndrome state with elevated fat mass, elevated cholesterol and triglycerides as well as dysregulated blood glucose. These rats have been bred out over 30 generations to have this drastic metabolic difference. Thirteen, mixed-sex HCR/LCR rats (HCR, n=7; LCR, n=6), between 6 to 9 months of age were used for this study. All animals were originally obtained from the University of Michigan and were housed in the Comparative Medicine Unit at Northeast Ohio Medical University (NEOMED) for the duration of this study. Animals were given free access to food and water, maintained on a 12-hour light/dark cycle, and all procedures were approved by the NEOMED Institutional Animal Care and Use Committee.

2.2. Intraocular Pressure (IOP) Measurements

Rats were anaesthetized using 2.5% isoflurane inhalant. A Tonolab was used to take 15 IOP measurements per eye; measurements were averaged together to get the daily IOP reading for each eye. IOPs were taken once a week, at the same time of day, for a total of four weeks to get a reliable baseline measure.

2.3. Immunohistochemistry in brain, retinal, and optic nerve sections

2.3.1. Preparation of Tissue Sections

Three rats from both the LCR group and the HCR group were anesthetized with a lethal dose of barbiturate anesthetic (*Beuthanasia D Special*, 200 mg/kg body weight, *i.p.*) and then transcardially perfused with phosphate-buffered saline (PBS, in mM: 137 NaCl, 2.7 KCl, 10 Na₂HPO₄, 1.8 KH₂PO₄, pH 7.4 at room temperature) and 4% paraformaldehyde (PFA) in PBS. Brains, optic nerves (ONs), and eyes were harvested. Brains and ONs were post-fixed overnight in 4% PFA, then transferred to a 20% cryoprotectant sucrose solution prior to slicing. Whole retinas were dissected from the eyeballs, were post-fixed for 2 hours, and then placed in PBS. The whole brain was sliced coronally at 50µm while ONs were sliced at 20µm, longitudinally, on a freezing microtome. Both the ON, brain slices, and whole retina were then placed in plates with wells full of PBS. These plates were stored under foil at 4°C until use.

2.3.2. Immunohistochemistry: ON and SC

For immunostaining, the ON, and Superior Colliculus (SC) slices were blocked between 1.5-2 hours in 5% normal serum (donkey) plus 1% of Triton X-100 10% stock solution diluted in PBS/azide. Then the tissue was incubated with primary antibodies anti-rabbit GFAP (*1:500 dilution, Z0334, DAKO, Santa Clara, California*) and anti-mouse AQ4 (*1:200 dilution, ab951, Abcam, Cambridge, UK*) at 4°C for two days. After 3, 10-minute washes in PBS, the secondary antibodies were added for 2 hours at room temperature. AlexaFluor secondary antibodies were used to visualize the markers. GFAP was stained with Donkey α Rabbit 594 (*Red, 1:250, Jackson Laboratories, 711-586-152, West Grove, PA*) and AQ4 was stained with Donkey α Mouse 488 (*Green, 1:250, 715-546-150, Invitrogen, Grand Island, NY*). The tissues were washed again 3 times for 10 minutes each wash. Fixed tissue slices of the SC were also treated with DAPI (*4',6-diamidino-2-phenylindole, basic cell nuclei marker*) after mounting; this was done to ensure that total cell counts did not differ between areas analyzed between animals and groups. The slices of ON and SC and were placed onto glass slides and coverslipped using Fluoromount-G (*Southern Biotech, Birmingham, AL*). Fluorescently stained sections were observed with a Zeiss Axiozoom V16 microscope attached to a CCD camera, with Zen 2011 software. Exposure times remained consistent for all tissue samples. For GFAP in the 594nm channel, the exposure time was 750ms and AQ4 in the 488nm channel the exposure time was 800ms. The objective used was a NeoFluar 2.3 objective.

2.3.3. Immunohistochemistry: Retina

Whole retinas were assayed while free-floating in a well plate. Tissues were blocked with a 5% normal donkey serum and 1% Triton-X 100 in PBS for 2 hours. Then tissues were incubated for 48 hours at 4°C in the following primary antibody cocktail (*diluted in 3% serum, 1% Triton in PBS*): rabbit polyclonal anti-GFAP (*1:500 dilution, DAKO, Z0334, Santa Clara, California*) and mouse monoclonal anti-AQ4 (*1:200 dilution, Abcam, ab9512, Cambridge, UK*). Following three 10 minute washes with PBS, secondary antibody cocktail was added for 2 hours at room temperature, which contained) donkey anti-rabbit Alexafluor 594 (*1:250, Jackson Laboratories, 711-586-152; West Grove, PA*) and donkey anti-mouse Alexafluor 488 (*1:250, Invitrogen, A-31571; Grand Island, NY*). Tissue was then rinsed three times with PBS, mounted and coverslipped with Fluoromount-G (*Southern Biotech, Birmingham, AL*).

Whole-mount retinas were photographed with a Zeiss Axioimager M2 epifluorescent microscope equipped with a digital high-resolution camera (*AxioCam MRm Rev.3; Zeiss, Jena Germany*) and a computer guided motorized X-Ystage. An apotome module (*Zeiss Apotome.2*) was used to collect z-stack of images using structured illumination. Images on the whole retina were focused on the ganglion cell layer as illustrated by Brn3a labelling, a retinal ganglion cell body marker. Exposure times remained consistent for all retina samples. For GFAP in the 594nm channel, the exposure time was 750ms and AQ4 in the 488nm channel the exposure time was 800ms. The objective used was a NeoFluar 2.3 objective.

2.4. Immunofluorescence quantification of brain, optic nerve slice, and retina

Quantitative analysis of GFAP intensity as well as percent area fraction (%GFAP staining/total area) were measured in the SC, ON, and retina. GFAP intensity corresponds to astrocyte reactivity. Percent area fraction was also used for AQ4 as well as a count of AQ4+ astrocytes. The intensity was calculated by using ImagePro Software while the percent area fraction was calculated with ImageJ Software.

2.5. Statistical Analysis

The statistical comparisons between the LCR rat and HCR rat tissue for Area, Intensity Mean Red (luminescence), Intensity Uncalibrated (luminescence), Max Intensity (luminescence), Mean Intensity (luminescence) and Intensity Standard Deviation (luminescence) from the intensity measurements were performed by using the unpaired student's t-test. Statistical Analyses were performed using Microsoft Excel software. Differences were deemed to be significant with p value < 0.05.

The statistical differences between the average percent-area fractions of GFAP in the LCR rats was compared to the HCR rats by using the unpaired student's t-test. The statistical analyses were performed using Microsoft Excel Software. Differences were deemed to be significant with p value < 0.05.

3. Results

3.1 No IOP differences between strain and gender

Baseline IOPs did not differ between animals based on strain or gender (**Figure 1**).

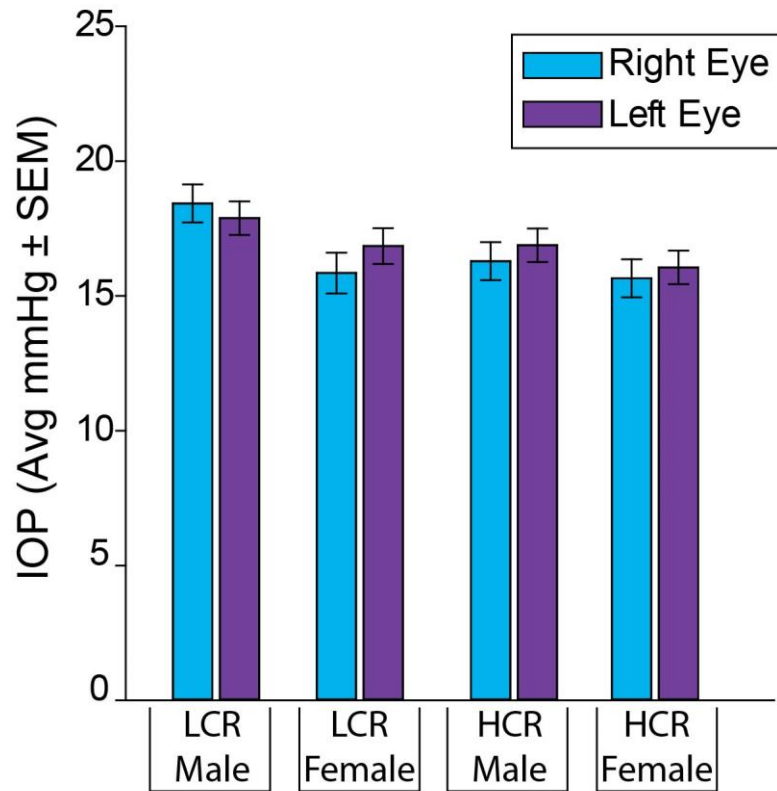


Figure 1: Baseline IOP based on strain and gender. No IOP differences between strain or gender, indicating that metabolic differences due to MetS status does not affect IOP.

3.2. GFAP is elevated in distal portions of LCR retinal projections compared to HCR projections

The astrocytic marker, GFAP, was quantified throughout the RGC projection of LCR/HCR rats, with the most striking differences being found within the SC. Overall, the data suggests more astrocytic staining within the SC of LCR compared to HCR rats, with differences in ON and retina not reaching statistically significant levels. Thus, the following findings point to early distal changes in inflammatory state within a metabolically-challenged RGC projection even prior to elevation in IOPs or similar changes within proximal portions of the projection (**Figure 1**).

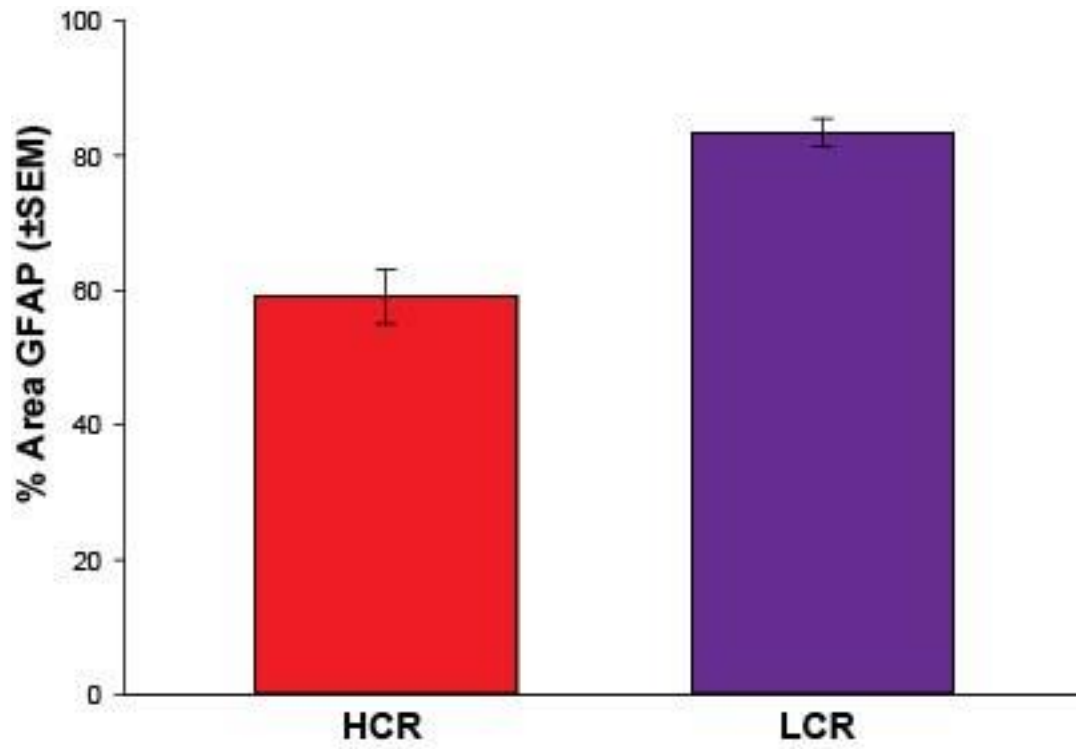


Figure 2: Percent-Area Fraction of GFAP. The percent-area GFAP in the Superior Colliculus is significantly greater in LCR compared to HCR rats. Error bars are standard error of the mean. $P < 0.05$.

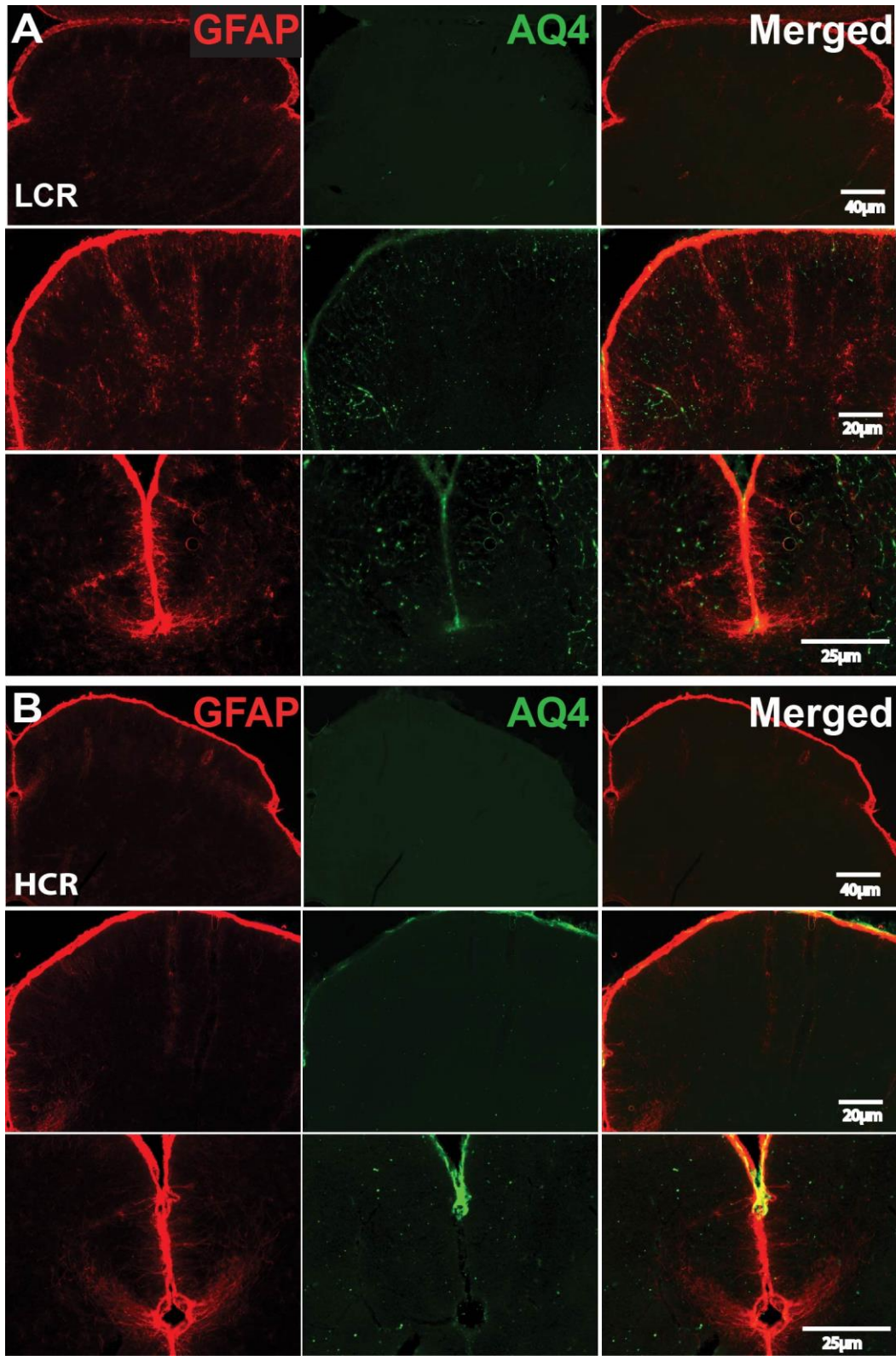


Figure 3: A. LCR rat Superior Colliculus Images at 32x, 63x, and 80x using an AzioZoom microscope. Take note of the increased staining of GFAP and AQ4. B. HCR Superior Colliculus

Images at 32x, 63x, and 80x using an AzioZoom macroscope. Take note of the decreased staining of GFAP and AQ4.

3.2.1. Differences in Retinal GFAP of LCR/HCR Rats

To examine the levels of reactive astrocytes, GFAP percent-area fraction measurements were used. The HCR rats had a mean percent-area fraction of 0.655 and the LCR rats had a mean percent-area fraction of 0.577, which did not suggest elevated GFAP in the retina of LCR rats compared to HCR rats, but did not reach statistical significance (**Figure 4A & B**).

Intensity values measured by Image Pro also indicated no significant differences between groups.

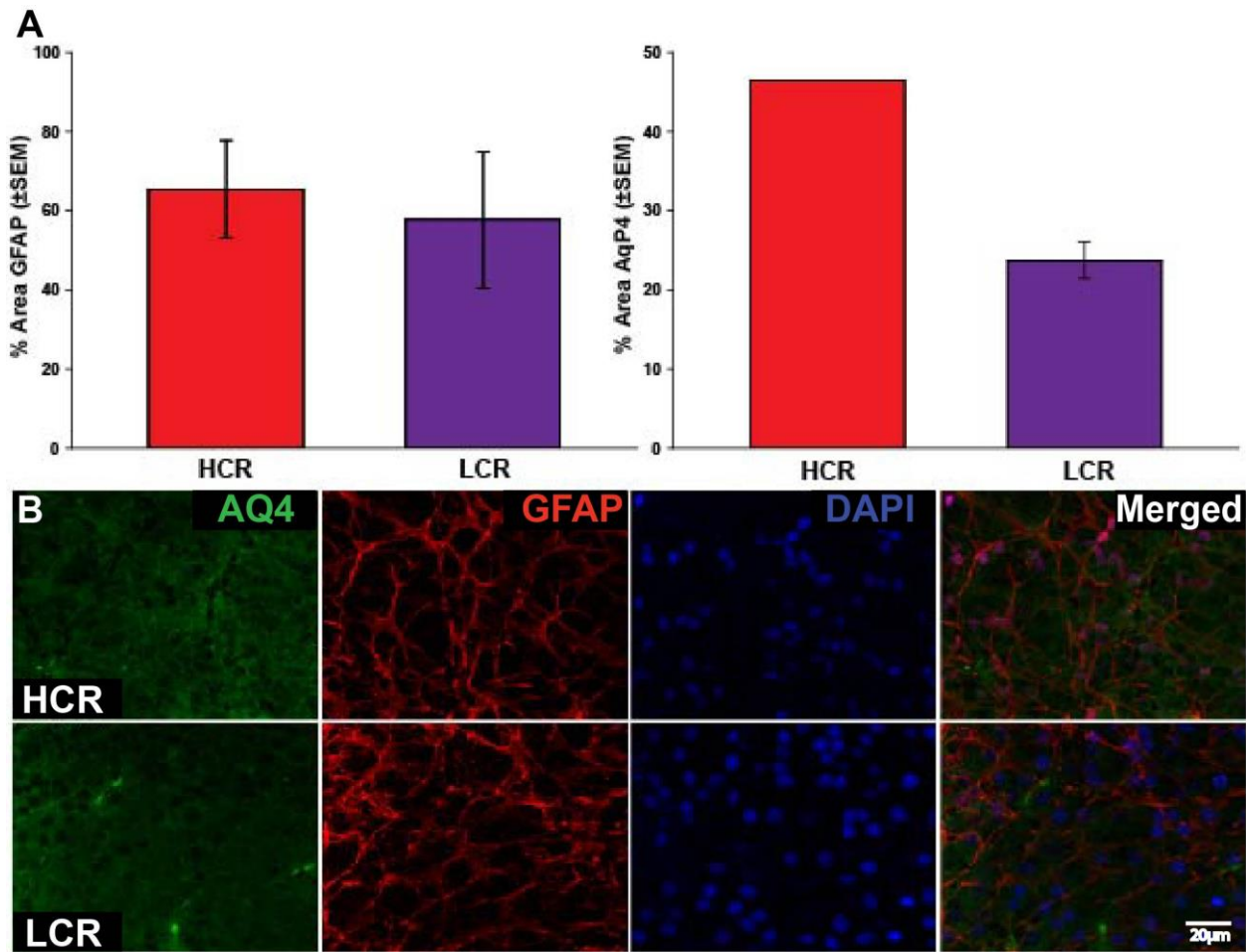


Figure 4: A. There was no significant difference in the staining of GFAP or AQ4 staining in the whole retina, due to the small sample size. Error bars are standard error of the mean. $P < 0.05$. B. HCR and LCR Retina imaged on an M2 Axioplan II microscope at 80x magnification. These images are focused on the ganglion cell layer of the retina.

3.2.2 Differences in Optic Nerve GFAP of LCR/HCR Rats

To examine levels of reactive astrocytes, GFAP and Aq4 intensity measurements were used in the ON. These measurements within the ON suggest elevated GFAP in the ON of LCR rats (mean intensity = 21.43) compared to HCR rats (mean intensity = 19.82) ($p = 0.06$), but this did not reach statistical significance (Table 1 in Appendix A).

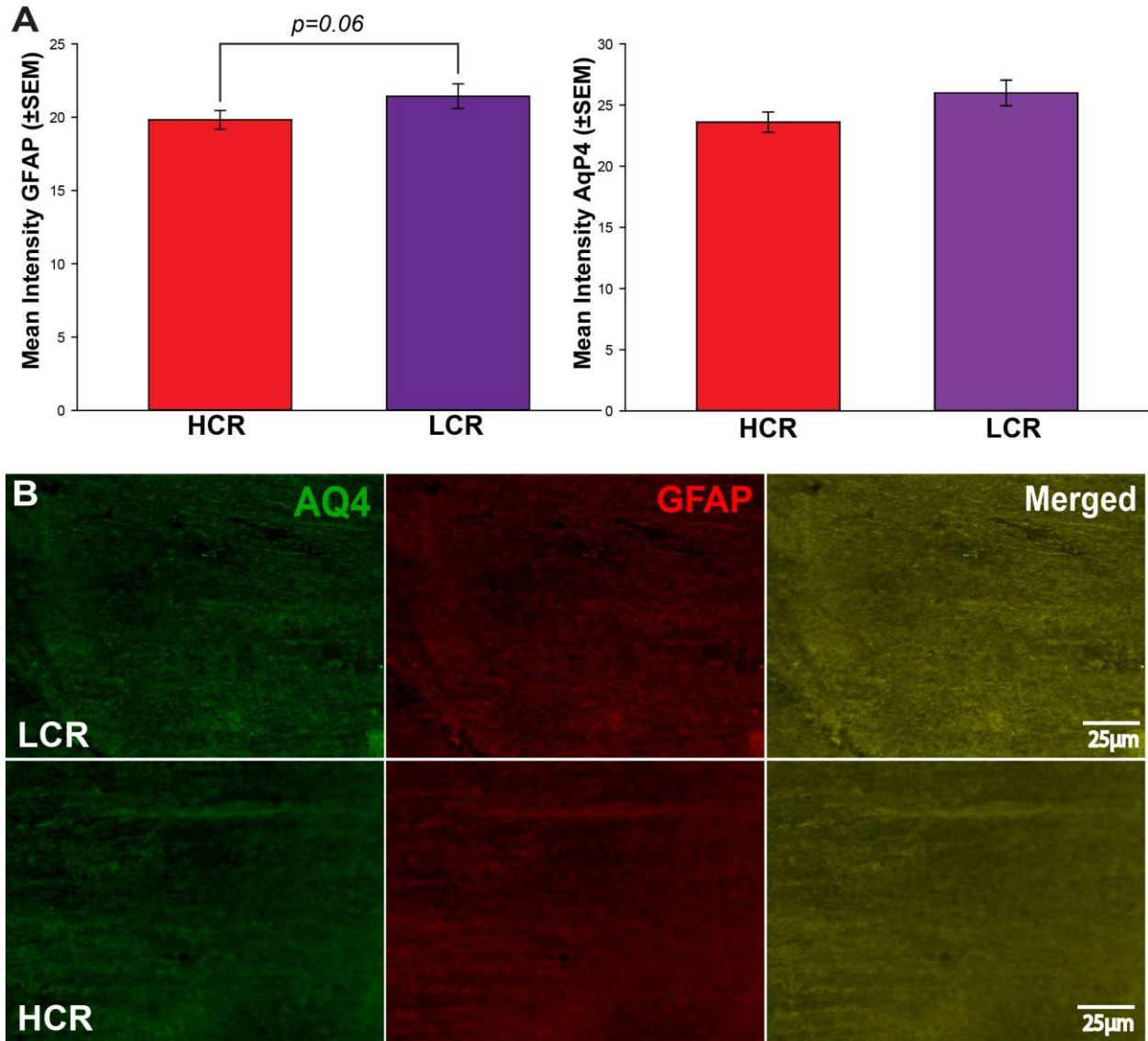


Figure 5: A. ON sections were displaying a trend toward increased GFAP intensity in LCR ON. ON sections were not analyzed using percent-area fraction. B. HCR and LCR ON imaged on an M2 Axioplan II microscope at 160x magnification.

3.2.3 Differences in Superior Colliculus GFAP of LCR/HCR Rats

Percent-area fraction measurements showed that LCR rats had significantly higher GFAP staining in the SC compared to LCR rats: LCR (**Figures 2 & 3**). Interestingly, intensity measurements showed the opposite effect, with GFAP intensity of HCR SC being significantly higher. However, this may be explained assay-specific differences.

3.3 Differences in AQ4 between HCR and LCR Rats.

3.3.1 Differences in AQ4 Intensity for the ON of LCR/HCR Rats

In the ON of the LCR/HCR rats, the LCR rats had significantly greater values for Intensity Uncalibrated (luminescence) and Mean Intensity (luminescence) than the HCR rats (**Figure 5A and B**).

3.3.2 Differences in AQ4 Intensity for the SC of LCR/HCR Rats

There was a significant difference in AQ4 found between the HCR/LCR rats, with LCRs having significantly more AQ4 expressed in their SC. Specifically, an elevation within HCRs was elucidated in measures of Area, Intensity Mean Green (luminescence), Intensity Uncalibrated (luminescence), Mean Intensity (luminescence) (**Table 2 in Appendix A**).

3.3.3. Differences in AQ4 Intensity for the Retina of LCR/HCR Rats

Although statistical analysis could not be run, as there was little to no AQ4 staining within the retina of either strain. **Figure 4** suggests that it may be qualitatively elevated in LCR retina.

3.4 No differences in GFAP or AQ4 observed in cerebellar control tissue

As expected, no significant differences were observed in mean intensity measures or percent-area fraction of GFAP or AQ4 in non-visual system tissue, indicating that aforementioned observations are at least partially specific to the retinal projection.

Please see appendix for more information on group averages and statistics for GFAP and AQ4 intensities and percent-area fractions.

4. Discussion and Conclusions

In this study, we were evaluating the differences in the regulation of GFAP and AQ4 in key areas of the retinal ganglion cell (RGC) projections (ON, SC, and retina) and other important thalamic nuclei in MetS rats for expression of GFAP and AQ4 of LCR/HCR rats. Neuroinflammation is a common factor in many pathological states, especially in the case of brain trauma or disease. LCR rats have a MetS phenotype and it has been reported that they have dysfunctional inflammation-resolving pathways (Su et al., 2012). However, little work has been done to characterize inflammatory markers within the central nervous system, and even less has been

done regarding visual system structures despite the fact that MetS comorbidities often include visual system dysfunction. Data from this study is important because it illustrates that there are not only astroglial differences within the central nervous system – and specifically, differences within important visual system structures. This research on the differences in the visual projections between the LCR and HCR groups could provide valuable insights to the progression of glaucoma pathology and its relationship to metabolism which could have a large impact for many humans suffering from Metabolic Syndrome.

We chose to be more confident in the findings from the Image J percent area fraction analysis vs. the intensity analysis done by ImagePro because in the other studies that have used GFAP intensity, the intensity analysis often times excluded differences in the number of GFAP-positive cells, which a percent area fraction measure can largely circumvent. Additionally, the results that were found with the ImageJ analysis were more consistent with the current literature available regarding the HCR/LCR rat model.

In this study, the intensity and percent area fraction results were very different (the HCR rats had significantly greater intensities of GFAP, but significantly lower percent area fractions of GFAP than the LCR rats did). This discrepancy could have been due to similar activation of astrocytes between groups as well as generally low numbers of astrocytes overall in tissue. This could have led to a greater emphasis on differences in background staining between animals, which would have also affected intensity measures as well as percent area fraction. We took this to mean that the LCR rats had a greater amount of astrocytes present that may have had lower intensity due to interference with the background.

It is also worthy to note that there was no significant differences in the retina of the LCR and HCR groups. This is probably due to either the size of the sample—we would need to run analysis with a larger amount of retina—or due to the fact that the pathology of glaucoma usually first manifests distally (in the SC) before appearing in the proximal ON or retina. Additionally, retinas already contain a higher amount of glia and astroglia under normal conditions, so detecting a difference may be more difficult. For example, Müller glia – which stain positive for GFAP – ensheath all retinal ganglion cell bodies within the retina (Bringmann et al., 2006).

To summarize, this study demonstrates that differences in metabolism, such as the case of the LCR/HCR rats, can lead to differences in the regulation of GFAP and AQ4, especially in the SC. These findings suggest that the metabolic differences between the two groups of rats led to the LCR rats having heightened levels GFAP and AQ4 within their visual structures, suggesting innate immune differences between the rat groups. Given what we know regarding glial reactivity and the role of glia in glaucoma and other visual system disorders, it would not be surprising to find functional vision differences between these strains or at least an increased susceptibility towards developing diseases such as glaucoma in the LCR animals. Furthermore, the observation of differences in the SC, more than other visual structures (i.e., retina and optic nerve), provides evidence that pathology can begin distally and therefore be asymptomatic until

damage has progressed and diagnosable signs of glaucoma and/or retinopathy become apparent in an eye exam – and at that point, damage is likely irreversible. Others have found that glaucomatous neurodegeneration, for example, is asymptomatic at first and that damage to retinal ganglion cell axons begins distally (near SC) (Crish et al., 2010).

For future study, it would be interesting to see if glaucoma-like pathology were to be induced with the microbead occlusion model (MOM) in the HCR/LCR rats if the HCR rats would be more resistant to the elevated intraocular pressure (IOP) than the LCR rats. In the HCR and LCR rats, the IOPs of these groups were not significantly different. In a paper by Baltan and colleagues in 2010, it was noted that age can determine a rat's susceptibility to axonal damage in the induced cases of IOP. If a rat was older, it would have more damage overall and more permeant damage to the visual pathway due to a lack of a compensatory mechanism (Baltan et al, 2010). From this research combined with the research of this paper, it would seem that the LCR rats lack a compensatory mechanism that HCR rats may have, because with the same levels of IOPs, the LCR rats are presenting with more inflammatory indicators.

Again, once we know if astrocyte status—associated with neuronal stress and inflammation—is different within the visual system based solely on metabolic differences between subjects, then we can conduct more specific research aimed at finding a target molecule or pathway that can be manipulated. This could potentially provide an avenue towards a future therapy against glaucoma or other optic neuropathies—including diabetic retinopathy, as well as some other obscure diseases such as Leber's hereditary optic neuropathy. Until this study, the LCR/HCR rats have not yet been used for eye research, when they could in fact provide a new and exciting model that may be more applicable to the human condition or provide important links between visual neurodegenerations and metabolism that are currently missing.

5. References

- Baltan, S., Inman, D.M, Danilov, CA, Morrison, RS, Calkins, DJ, & Horner, PJ (2010). Metabolic vulnerability disposes retinal ganglion cell axons to dysfunction in a model of glaucomatous degeneration. *The Journal of Neuroscience : The Official Journal of the Society for Neuroscience*, 30(16), 5644–5652.
<http://doi.org.lib.ezproxy.uakron.edu:2048/10.1523/JNEUROSCI.5956-09.2010>
- Bringmann A, Pannicke T, Grosche J, Francke M, Wiedemann P, Skatchkov SN, Osborne NN, Reichenbach A (2006). Müller cells in the healthy and diseased retina. *Progress in Retinal and Eye Research*, 25, 397-424. Retrieved August 25, 2015 from <http://www.sciencedirect.com/science/article/pii/S1350946206000164#>
- Bondan, EF, Martins, MFM, & Viani, FC (2013). Decreased astrocytic GFAP expression in streptozotocin-induced diabetes after gliotoxic lesion in the rat brainstem. *Arquivos Brasileiros de Endocrinologia & Metabologia*, 57(6), 431-436. Retrieved August 12, 2015, from http://www.scielo.br/scielo.php?script=sci_arttext&pid=S0004-27302013000600004&lng=en&tlng=en. 10.1590/S0004-27302013000600004.
- Bouret SG, Draper SJ, & Simerly RB (2004). Formation of Projection Pathways from the Arcuate Nucleus of the Hypothalamus to Hypothalamic Regions Implicated in the Neural Control of Feeding Behavior in Mice. *The Journal of Neuroscience* 24(11): 2797-2805.
- Ceccariglia S, D'altocolle A, Del Fa A, Silvestrini A, Barba M, Pizzolante F, Repele A, Michetti F, Gangitano C (2014). Increased expression of aquaporin 4 in the rat hippocampus and cortex during trimethyltin-induced neurodegeneration. *Neuroscience*, 274: 273-288.
- Coleman AL & Kodjebacheva G (2009). Risk factors for glaucoma needing more attention. *The Open Ophthalmology Journal*, 3: 38-42.
- Crish SD, Sappington RM, Inman DM, Horner PJ, Calkins DJ (2010). Distal axonopathy with structural persistence in glaucomatous neurodegeneration. *Proc Natl Acad Sci USA*, 107(11): 5196-5201.
- DeMarco, VG, Johnson, MS, Ma, L, Pulakat, L., Mugerfeld, I, Hayden, MR., ... Sowers, J R (2012). Overweight female rats selectively breed for low aerobic capacity exhibit increased myocardial fibrosis and diastolic dysfunction. *American Journal of Physiology - Heart and Circulatory Physiology*, 302(8), H1667–H1682.
<http://doi.org.lib.ezproxy.uakron.edu:2048/10.1152/ajpheart.01027.2011>
- Koch LG & Britton SL (2001). Artificial selection for intrinsic aerobic endurance running capacity in rats. *Physiol. Genomics*, 5:45-52.

- Koch LG, Britton SL & Wisloff U (2012). A rat model system to study complex disease risks, fitness, aging, and longevity. *Trends Cardiovasc Med*, 22:29-34.
- Morris ME, Jackman, MR, Johnson, GC, Liu TW, Lopez JL, KearneyM L, ... Thyfault JP (2014). Intrinsic aerobic capacity impacts susceptibility to acute high-fat diet-induced hepatic steatosis. *American Journal of Physiology - Endocrinology and Metabolism*, 307(4), E355–E364. <http://doi.org.lib.ezproxy.uakron.edu:2048/10.1152/ajpendo.00093.2014>
- Nagelhus EA, & Ottersen OP (2013). Physiological Roles of Aquaporin-4 in Brain. *Physiological Reviews*, 93(4), 1543–1562. <http://doi.org.lib.ezproxy.uakron.edu:2048/10.1152/physrev.00011.2013>
- Novak CM, Escande C, Gerber SM, Chini EN, Zhang M, Britton SL, ... Levine JA (2009). Endurance Capacity, Not Body Size, Determines Physical Activity Levels: Role of Skeletal Muscle PEPCK. *PLoS ONE*, 4(6), e5869. <http://doi.org.lib.ezproxy.uakron.edu:2048/10.1371/journal.pone.0005869>
- Su X, Feng X, Terrando N, Yan Y, ChawlaA, Koch LG, Britton SL, Matthey MA, Maze M (2012). Dysfunction of inflammation-resolving pathways is associated with exaggerated postoperative cognitive decline in a rat model of the metabolic syndrome. *Mol Med*, 018(1): 1481-1490.

6. Appendix A: Supplementary Tables

GFAP-Superior Colliculus	Mean intensity (Red)	Intensity Max (lum)	Mean Intensity	Std Dev
HCR (SC)	28.55	85.97	9.73	8.45
LCR (SC)	21.13	86.86	7.20	5.65
p-value	0.04201	0.3217	0.0426	0.0454

Table 1: GFAP Intensity in SC for HCR and LCR Rats

AQ4-Superior Colliculus	Mean intensity (Green)	Intensity Max (lum)	Mean Intensity	Std Dev
HCR (SC)	21.15	47.24	8.15	4.87
LCR (SC)	10.34	41.29	3.91	0.66
p-value	0.02968	0.3236	0.0361	0.040

Table 2: AQ4 Intensity in SC for HCR and LCR Rats

GFAP-Optic Nerve	Mean intensity (Red)	Intensity Max (lum)	Mean Intensity	Std Dev
HCR (ON)	58.82	63.48	19.82	4.53
LCR (ON)	63.53	62.22	21.43	4.15
p-value	0.06733	0.4057	0.06400	0.121

Table 3: GFAP Intensity in ON for HCR and LCR Rats

